Melting and Sintering of a Body-Centered Cubic PbSe Nanocrystal Superlattice Followed by Small Angle X-ray Scattering

Brian W. Goodfellow[a], *Reken N. Patel*[a], *Matthew G. Panthani*[a], *Detlef-M. Smilgies*[b], *Brian A. Korgel*[a,*]

[a]Department of Chemical Engineering, Texas Materials Institute, Center for Nano- and Molecular Science and Technology, The University of Texas at Austin, Austin, Texas 78712-1062

[b]Cornell High Energy Synchrotron Source (CHESS), Cornell University, Ithaca, New York 14853

* Corresponding author: korgel@che.utexas.edu; (T) 512-471-5633; (F) 512-471-7060.

Supporting Information

Table 1 summarizes the superlattice *d*-spacings determined by TEM and SAXS. Good agreement exists between the measurements. In the SAXS data, reflections that would correspond to odd values of the quantity *h*+*k*+*l* do not appear, as they are forbidden for bcc lattices.

Table S1. Comparison of bcc superlattice *d*-spacings determined by TEM and SAXS.

	d(hkl) (nm)	
(hkl)	from TEM	from SAXS
(100)	10.57	
(110)	7.63	7.61
(111)	6.14*	
(200)	5.32*	5.44
(210)	4.71	
(211)	4.34*	4.40
(220)	3.76*	3.80
(300),(221)	3.54*	

* These values were calculated from the average lattice constant of $a_{bcc,TEM} = 10.63\,\text{nm}$ determined from the *d*(100), *d*(110), and *d*(210) spacings observed by TEM.

Figures S1-S3 show thermaogravimetric analysis (TGA) data for pure oleic acid and 9 nm diameter oleic acid-capped PbSe nanocrystals. Figure S2 shows a magnification of the lower temperature weight loss from the nanocrystal sample to highlight the amount of weight loss due to solvent evaporation. Figure S4 shows the differential scanning calorimetry (DSC) data collected simultaneously with the TGA scan of pure oleic acid and the oleic acid-capped PbSe nanocrystals. The endothermic peaks for the oleic acid scans correspond to evaporation of the pure ligand. The exothermic peak observed for the nanocrystals corresponds to the sintering temperature when there is a significant loss of PbSe surface area due to particle fusion.

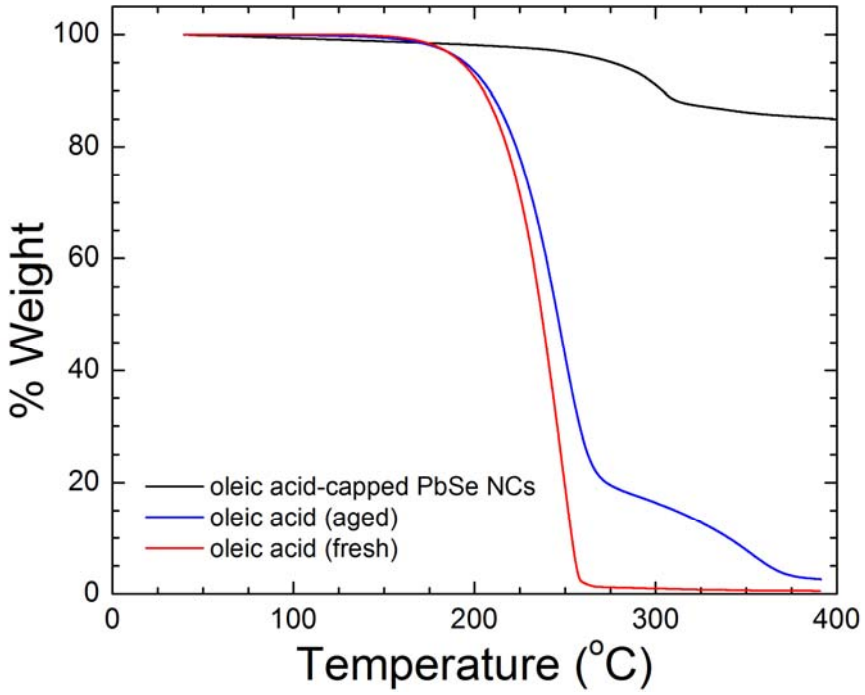

Figure S1: Thermogravimetric analysis (TGA) of oleic acid-capped 9 nm diameter PbSe nanocrystals and pure oleic acid. Data were collected for oleic acid immediately after receiving it from the supplier and after storing for one month in the laboratory at room temperature in ambient atmosphere. A ramp rate of 3°C/min was used, which was identical to that used in the in situ SAXS experiments.

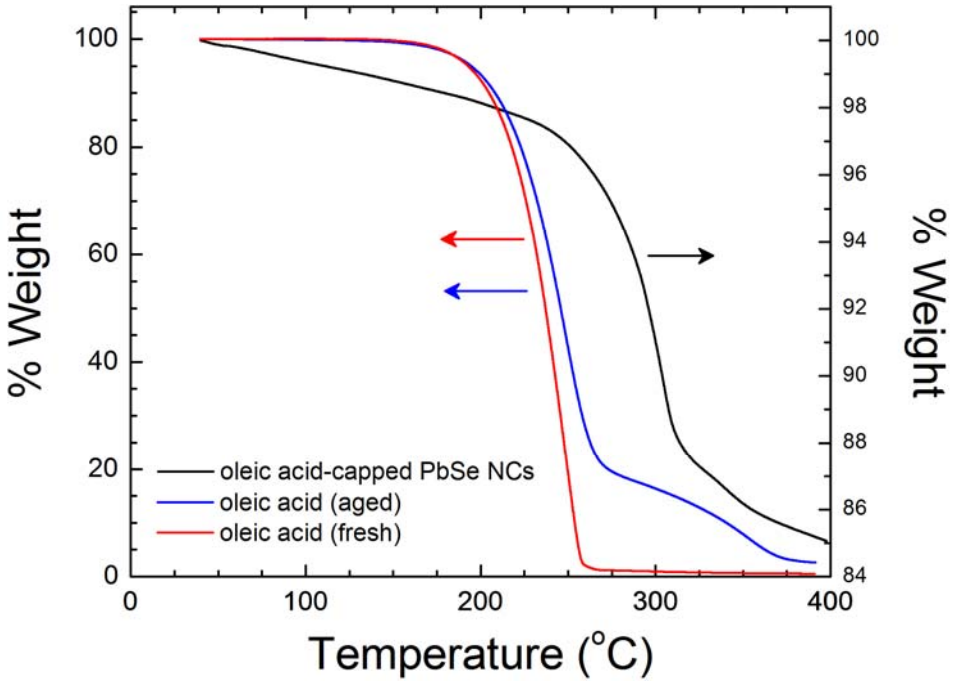

Figure S2: The TGA data from Figure S1 plotted with the oleic acid-capped PbSe nanocrystals on a different scale to highlight the amount of weight loss at the lower temperatures.

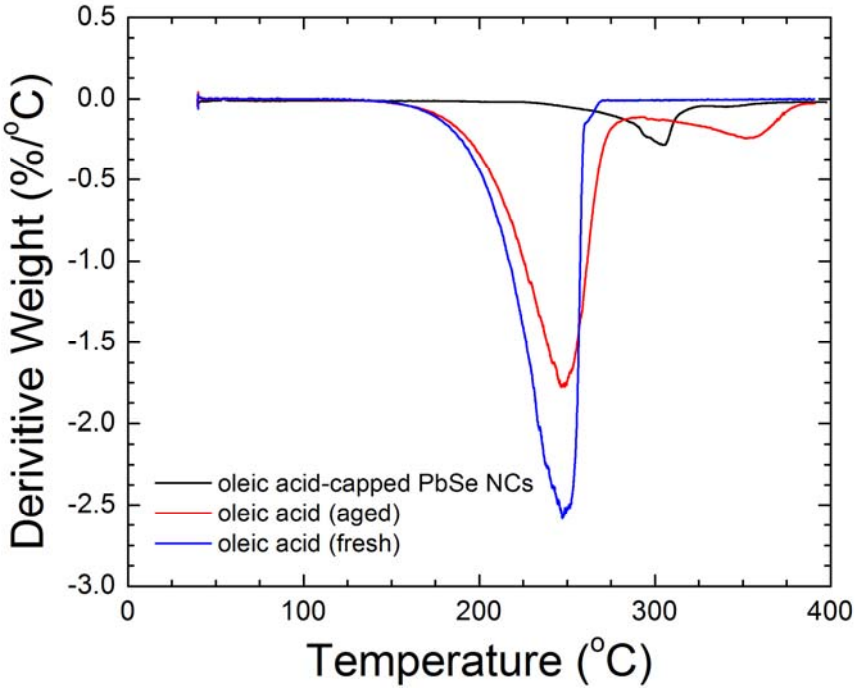

Figure S3: Derivatives of the TGA weight loss curves in Figure S1. Pure oleic acid begins to evaporate at about 150°C, whereas oleic acid adsorbed to the PbSe nanocrystals surface evaporates at higher temperature.

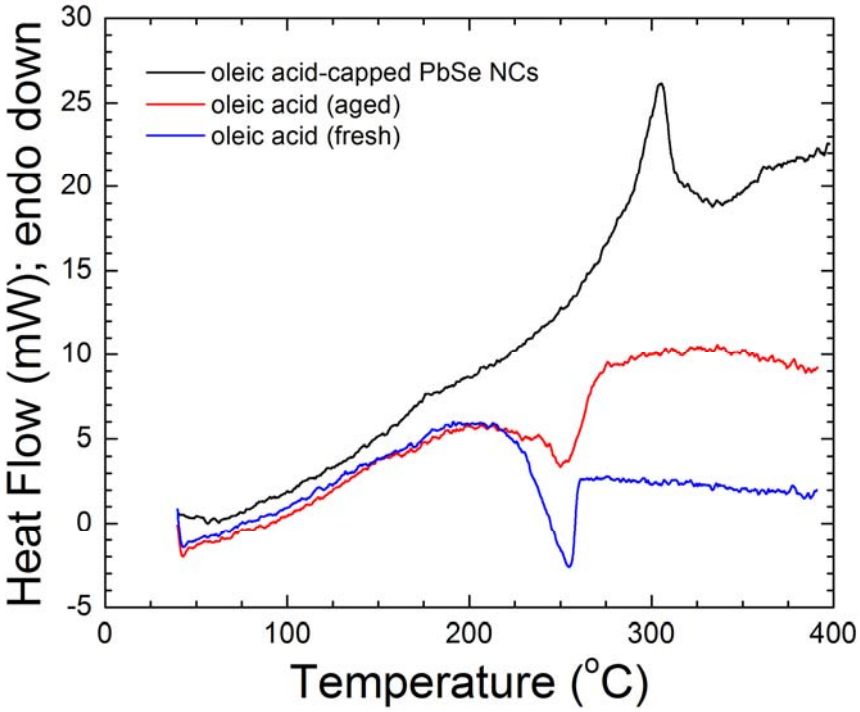

Figure S4: Differential Scanning Calorimetry (DSC) curves for oleic acid-capped PbSe nanocrystals and pure oleic acid. The oleic acid curves exhibit an endothermic peak near 250°C associated with the evaporation of oleic acid. The PbSe nanocrystals exhibit an exothermic peak at 300°C attributed to sintering and oxidation.

Figures S5-S7 show additional TEM images of PbSe nanocrystals. Figure S5 shows TEM images of 9 nm diameter oleic acid-capped PbSe nanocrystals before and after heating in air to 300°C. The PbSe nanocrystals oxidize and transform into $PbSeO_3$ nanorods. The $PbSeO_3$ composition was confirmed by XRD, as discussed in the main body of the manuscript. Figure S6 shows high resolution TEM images of a bcc superlattice of PbSe nanocrystals taken to determine if there is registry between the crystallographic orientation of the nanocrystals in the superlattice. The corresponding FFTs of the images do not appear to exhibit a correlation of crystallographic orientation between neighboring nanocrystals. Figure S7 shows high resolution TEM images of a bcc superlattice of 6.6 nm diameter oleic acid-capped PbSe nanocrystals obtained at varying focal depth.

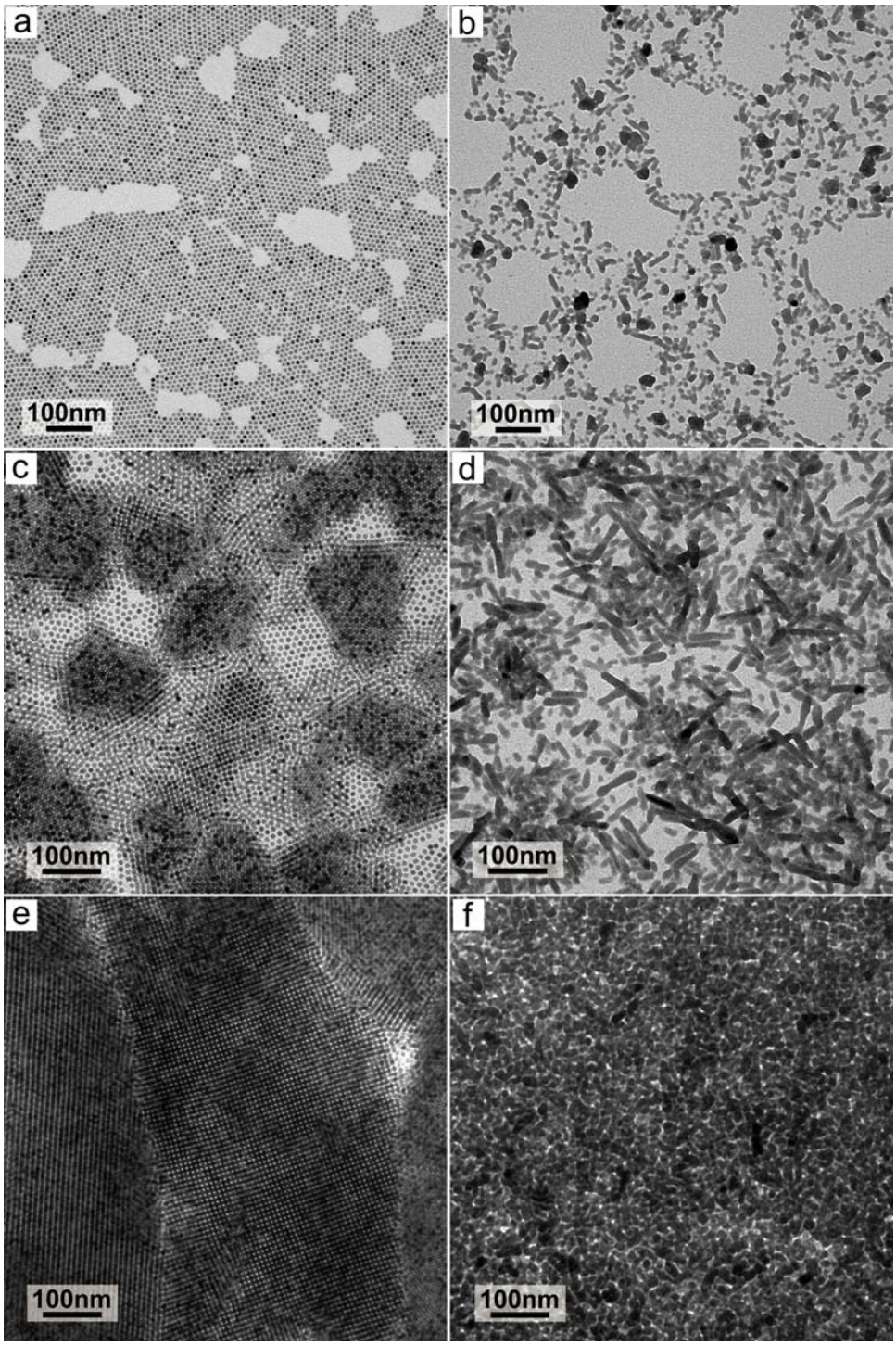

Figure S5: TEM images of 9 nm diameter oleic acid-capped PbSe nanocrystal superlattices at room temperature (a,c,e) and after heating to 300°C in air (b,d,f). The PbSe nanocrystals oxidize and convert to $PbSeO_3$ nanorods when heated to 300°C in air.

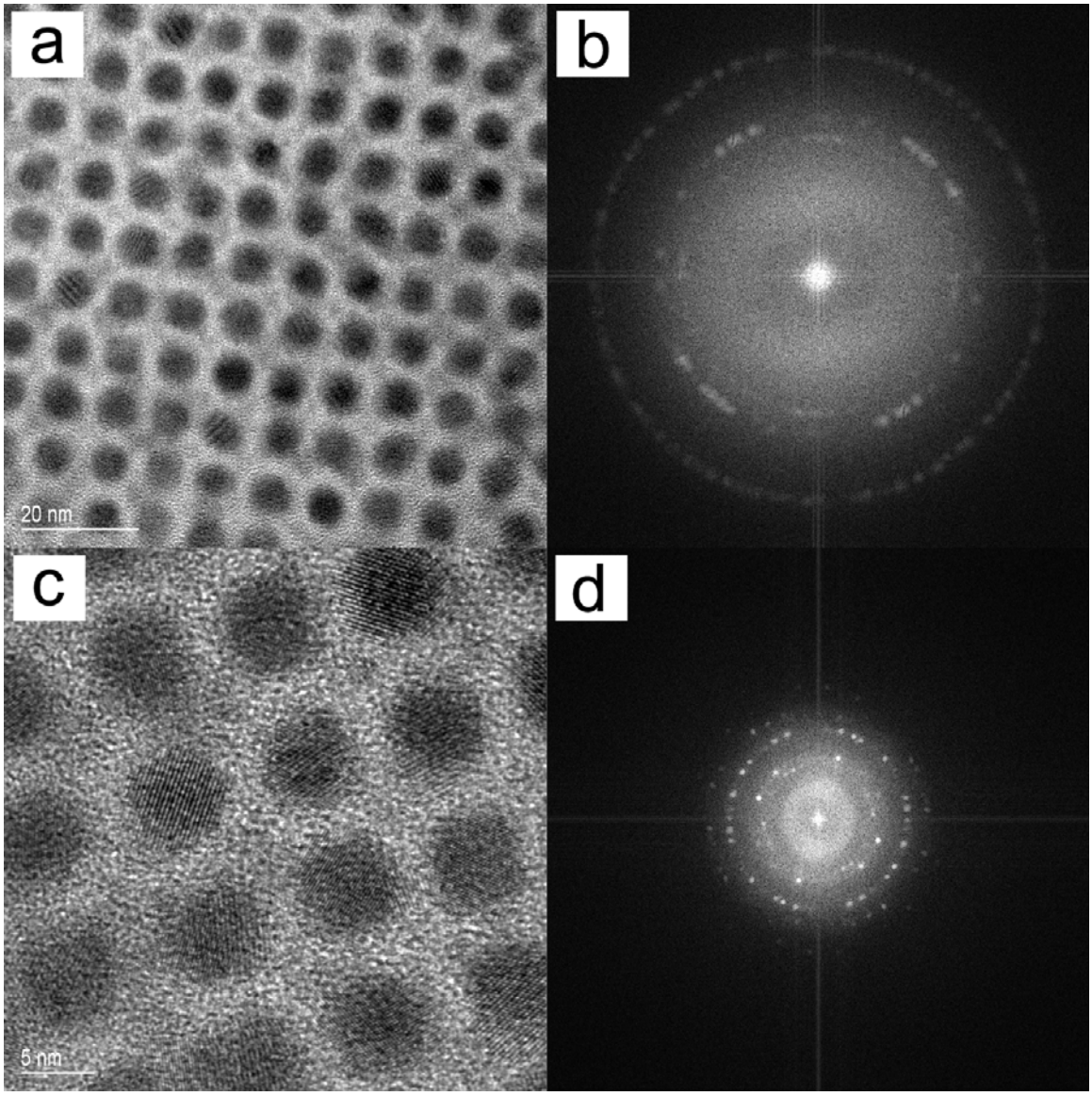

Figure S6: (a,c) High resolution TEM images and (b,d) corresponding FFTs of a bcc superlattice of 6.6 nm diameter oleic acid-capped PbSe nanocrystals. From this data, a preferential crystallographic orientation of the nanocrystals does not appear to occur.

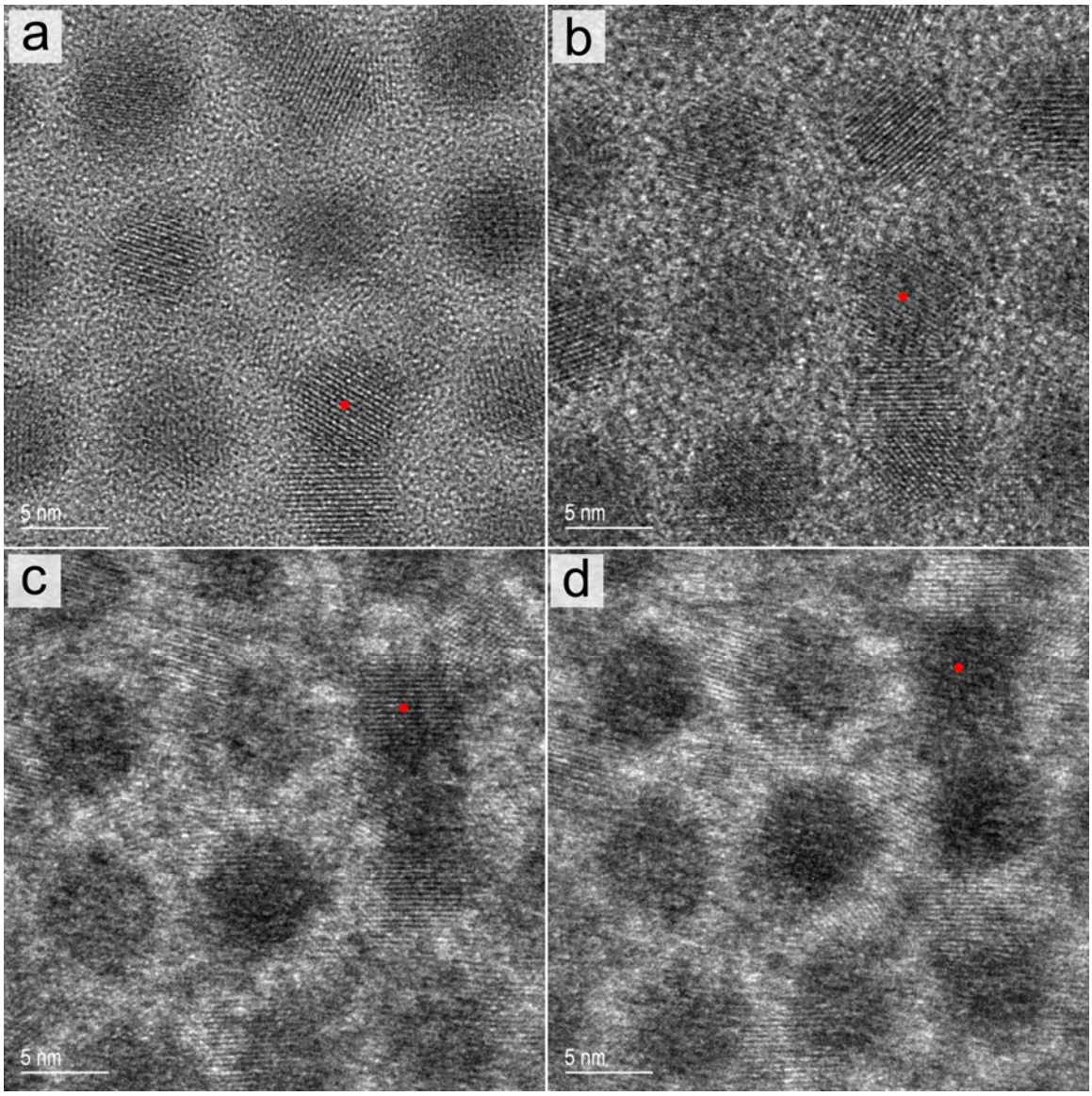

Figure S7: High resolution TEM images of a bcc superlattice of 6.6 nm diameter oleic acid-capped PbSe nanocrystals as the focal depth was increased. Beginning with the focused image in (a), the focal depth was gradually increased in the images (b-d), revealing lattice fringes of the underlying nanocrystal layers. The red dots in the images mark the same spot in the superlattice.